Recognition of dicarboxylate anions by a ditopic hexaazamacrocycle containing bis-*p*-xylyl spacers

Sílvia Carvalho,[a] Rita Delgado,*[ab] Nelson Fonseca[c] and Vítor Félix*[c]

Received (in Durham, UK) 7th September 2005, Accepted 8th December 2005
First published as an Advance Article on the web 11th January 2006
DOI: 10.1039/b512661d

The hexaprotonated form of the hexaazamacrocycle, 7,22-dimethyl-3,7,11,18,22,26-hexaazatricyclo[26.2.2.2.13.16]tetratriaconta-1(30),13,15,28,31,33-hexaene, $(H_6Me_2[30]pbz_2N_6)^{6+}$, was used as a receptor for the molecular recognition of aliphatic and aromatic carboxylate substrates. The receptor–substrate binding behaviour of $(H_6Me_2[30]pbz_2N_6)^{6+}$ with aliphatic $> {}^{-}O_2C(CH_2)_nCO_2{}^{-}$, $n = 0$ to 4] and aromatic (benzoate, phthalate, isophthalate, and terephthalate) substrates was evaluated by potentiometry and ^{1}H NMR spectroscopy. The association constants of the entities formed were determined in H_2O at 298.0 K and 0.1 M KNO_3 (by potentiometry) and in D_2O (by ^{1}H NMR). The constants for the aliphatic substrates are much lower than for the aromatic ones. NMR spectroscopy allowed the conclusion that the recognition process might involve H-bonding, electrostatic and π–π stacking interactions, the strength and the type of them depending on the substrate. The cooperative conjugation of the three types of interactions only occurs when terephthalate is the substrate. Molecular dynamics simulations (MD) in a periodic box of water solvent molecules were also used to investigate the nature of the binding association between the receptor and the three aromatic dicarboxylate anions (phthalate, isophthalate, and terephthalate). These studies confirmed that the $(H_6Me_2[30]pbz_2N_6)^{6+}$ receptor encapsulates the terephthalate anion with the formation of an inclusion supermolecule stabilized by multiple N–H···O hydrogen bonding and π–π interactions. The molecular recognition between the receptor and the other two aromatic anions, phthalate and isophthalate, also occurs *via* N–H···O hydrogen bonds, but outside of the macrocyclic cavity. The results are discussed in terms of energetic and entropic contributions and showed that the binding association between the receptor and these anions is favourable.

Introduction

The importance played nowadays by anions in a variety of fields, such as the environment, the health and the industry is well known. For instance, the dicarboxylate anion adipate is a raw material in the nylon industry, and phthalic acid is used in the manufacture of paper, cosmetics, plastics, dyes and paints. Many anions are pollutants for the environment.

However due to the anion characteristics its recognition process is much more difficult than that of metal ions. Indeed, anions have larger sizes when compared with the isoelectronic metal ions, also they have a great variety of shapes and geometries, high free energies of solvation and they are pH dependent. Additionally the interactions involved in the association process are non-covalent (electrostatic, π–π stacking, H-bonding, *etc.*). Then the preorganization of the receptor is an important feature in order to achieve a strong or selective association. Receptor–substrate binding site complementarity and solvation effects are factors that must be taken into account in the design of a receptor.[1–5]

The macrocycle $Me_2[30]pbz_2N_6$ (L) contains six amine groups separated by propyl chains, which are long enough to allow the protonation of all the amine groups at pH ≈ 6, see Scheme 1. It is also expected that the presence of the two aromatic spacers in the receptor architecture should contribute to its rigidity, favouring the preorganization of the interacting groups, and to the decrease of its solvation, turning out the receptor appropriate for the recognition of difunctional anions. In the present work the hexaprotonated macrocycle $(H_6Me_2[30]pbz_2N_6)^{6+}$ was evaluated as a receptor for the binding of different dicarboxylate anions (aliphatic and aromatic) and also benzoate, by potentiometry and ^{1}H NMR spectroscopy in solution (see Scheme 2 for the studied anions). For a further insight into the nature of the binding between the receptor and three aromatic dicarboxylate anions, molecular dynamics simulations in periodic boxes of water solvent molecules were also carried out.

[a] *Instituto de Tecnologia Química e Biológica, UNL, Apartado 127, 2781-901 Oeiras, Portugal. E-mail: delgado@itqb.unl.pt; Fax: +351-214 41 12 77; Tel: +351-214 46 97 37/8*
[b] *Instituto Superior Técnico, Av. Rovisco Pais, 1049-001 Lisboa, Portugal*
[c] *Departamento de Química, CICECO, Universidade de Aveiro, 3810-193 Aveiro, Portugal. E-mail: vfelix@dq.ua.pt*

Results and discussion

Potentiometric measurements

The protonation constants of $Me_2[30]pbz_2N_6$ were determined by potentiometry in water, at 298.0 K and in 0.1 M KNO_3,

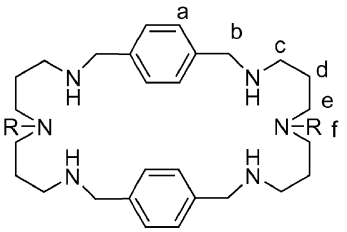

R - CH_3 $Me_2[30]pbz_2N_6$

R - H $[30]pbz_2N_6$

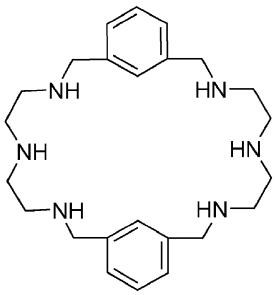

$[24]mbz_2N_6$

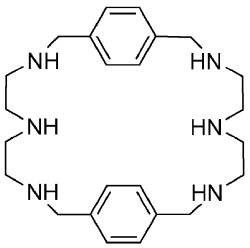

$[26]pbz_2N_6$

Scheme 1

and are collected in Table 1 together with the constants of the related compound without the methyl substituents, $[30]pbz_2N_6$.[6–8]

All the amine groups of both macrocycles are protonated at pH ≈ 6, and then these compounds exhibit a high overall basicity, see Table 1. The two values shown for each protonation constant of both compounds present some deviations, more significant for the first two values, which can be attributed to differences in the salt used to maintain the ionic strength, and also to problems associated with their low solubility in water.

The presence of the methyl groups on the central nitrogen atoms in $Me_2[30]pbz_2N_6$ reduces the basicity slightly and lowers the hydration of the corresponding amine groups in aqueous solution. The latter effect favours anion binding by attenuating the competitive interaction with solvent molecules.[9]

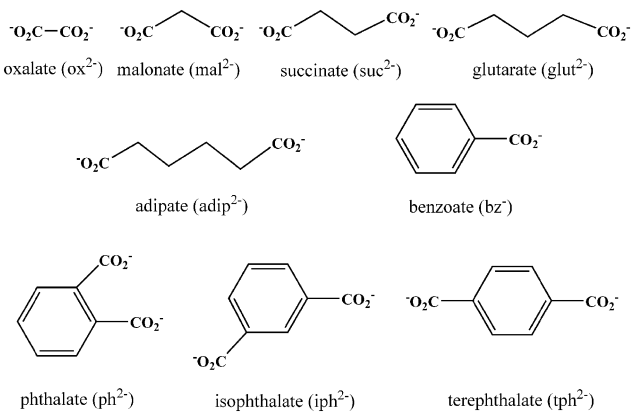

Scheme 2

Table 1 Protonation constants (log K_i^H) of $Me_2[30]pbz_2N_6$ and $[30]pbz_2N_6$ (T = 298.0 K; I = 0.10 mol dm^{-3} in KNO_3)

Equilibrium quotient	$Me_2[30]pbz_2N_6$		$[30]pbz_2N_6$	
$[HL]/[L] \times [H]$	9.99(1)[a]	10.41[b]	9.99[c]	10.55[d]
$[H_2L]/[HL] \times [H]$	9.59(1)[a]	9.82[b]	9.92[c]	10.06[d]
$[H_3L]/[H_2L] \times [H]$	8.47(1)[a]	8.82[b]	8.43[c]	8.56[d]
$[H_4L]/[H_3L] \times [H]$	7.67(1)[a]	7.87[b]	7.68[c]	7.67[d]
$[H_5L]/[H_4L] \times [H]$	6.66(1)[a]	6.79[b]	6.75[c]	7.12[d]
$[H_6L]/[H_5L] \times [H]$	6.21(1)[a]	6.27[b]	6.42[c]	6.70[d]
$[H_6L]/[L] \times [H]^6$	48.59(1)[a]	49.98[b]	49.19[c]	50.64[d]

[a] This work; values in parentheses are standard deviations on the last significant figures. [b] I = 0.1 mol dm^{-3} in KCl, ref. 6. [c] T and I are not indicated, ref. 7. [d] I = 0.1 mol dm^{-3} in KCl, ref. 8.

Binding of anions by $(H_6Me_2[30]pbz_2N_6)^{6+}$

Potentiometric studies. The association constants of $(H_6Me_2[30]pbz_2N_6)^{6+}$ with several dicarboxylate anions differing in shape, size and rigidity, such as aliphatic [oxalate (ox^{2-}), malonate (mal^{2-}), succinate (suc^{2-}), glutarate ($glut^{2-}$) and adipate ($adip^{2-}$)] and aromatic anions [phthalate (ph^{2-}), isophthalate (iph^{2-}) and terephthalate (tph^{2-})], were determined in aqueous solutions at 298.0 K and 0.10 mol dm^{-3} KNO_3 using the HYPERQUAD program.[10] Benzoate (bz^-), was also studied for comparison purposes. The values obtained are collected in Table 2. Due to solubility reasons, the protonation constants of tph^{2-} could not be determined with the necessary accuracy, and then the association constants of the receptor with this anion are not available by this technique, however it was possible to obtain the constants by ^1H NMR spectroscopy, see below.

As the protonation constants of the anionic substrates contribute significantly to the final association constants and the values from the literature exhibit large discrepancies,[11] those values were also determined in our experimental conditions and are shown in Table 3.

Only species of 1 : 1 receptor to anion stoichiometry were found for all the cases, although several species in which the receptor presents different protonation states were determined. In Table 4 the stepwise constants and the corresponding equilibrium reactions are compiled. For the aliphatic series only two or three species were found while for the aromatic substrates five or six different constants were determined. As expected the H_6LA^{4+} species exhibits the highest value, which corresponds to the association of the entirely protonated receptor and the deprotonated substrate, for which the strongest electrostatic interactions and the maximum number of hydrogen bonds should be formed. The H_7LA^{5+} species resulting from the self-association of H_6L^{6+} and the monoprotonated anion, HA^-, was also found in most of the cases, although with lower constants due mainly to weaker electrostatic interactions.

In Fig. 1 and 2 are shown the speciation diagrams corresponding to ox^{2-} and ph^{2-} substrates where the differences arising from the stronger binding of the aromatic substrates compared to the aliphatic ones can be visualized. As the constants for the associated entities involving the aromatic anions have larger magnitude, they resist higher at pH values

Table 2 Overall stability constants (log $\beta_{H_hL_lA_a}$)[a] for the equilibria of $(H_6[30]pbzN_6)^{6+}$ with ox^{2-}, mal^{2-}, suc^{2-}, $glut^{2-}$, $adip^{2-}$, ph^{2-}, iph^{2-}, and bz^-. L is the macrocyclic ligand $Me_2[30]pbzN_6$ and A the anion. I = 0.10 mol dm^{-3} in KNO_3 at 298.0 K

Equilibrium process	ox^{2-}	mal^{2-}	suc^{2-}	$glut^{2-}$	$adip^{2-}$	ph^{2-}	iph^{2-}	bz^-
$7H^+ + L + A^{2-} \rightleftarrows H_7LA^{5+}$	54.54(6)	—	—	55.31(7)	55.45(6)	56.12(5), 56.07(2)[b]	55.30(4), 55.34(3)[b]	55.58(5)
$6H^+ + L + A^{2-} \rightleftarrows H_6LA^{4+}$	51.30(2)	50.80(2)	50.82(8)	50.78(3)	50.65(4)	51.74(3), 51.80(1)[b]	51.64(2), 51.44(1)[b]	51.53(4)
$5H^+ + L + A^{2-} \rightleftarrows H_5LA^{3+}$	44.43(9)	43.99(9)	44.22(6)	44.46(5)	—	45.40(5), 45.34(1)[b]	45.27(3), 44.97(3)[b]	45.26(4)
$4H^+ + L + A^{2-} \rightleftarrows H_4LA^{2+}$	—	—	37.36(8)	37.40(9)	—	38.41(5), 38.38(2)[b]	38.48(3), 38.12(5)[b]	38.54(4)
$3H^+ + L + A^{2-} \rightleftarrows H_3LA^+$	—	—	—	—	—	30.35(9), 30.56(2)[b]	30.51(4), —	—
$2H^+ + L + A^{2-} \rightleftarrows H_2LA$	—	—	—	—	—	—, 21.45(7)[b]	21.77(5), —	—

[a] Values in parentheses are standard deviations on the last significant figures. [b] This work, I = 0.10 mol dm^{-3} in KCl.

in spite of the lower charge of the receptor, due to the successive deprotonation of the ammonium groups. Among the aliphatic substrates ox^{2-} exhibits the largest association constants, decreasing the strength of the binding with the increase of the methylenic chain (n) between the two carboxylate groups, $^-O_2C(CH_2)_nCO_2^-$. In Fig. 1 it is possible to observe that $H_7L(ox)^{5+}$ has its maximum value at pH about 2.5, while the main species $H_6L(ox)^{4+}$ reaches its maximum concentration at about pH 5, and $H_5L(ox)^{3+}$ is formed in very small amounts between pH 5.5 and 7.5. At higher pH values no assembled species remain, the receptor being successively in the forms H_4L^{4+}, H_3L^{3+},..., L, and the ox^{2-} in its free-state. In Fig. 2 it can be seen that the main species, $H_6L(ph)^{4+}$, exhibits its maximum percentage at pH $\approx$ 5.5, then other assembled species with successively lower charge are formed till pH about 10, overlapped by the corresponding protonated forms of the free ligand and the free ph^{2-} anion.

Another point that must be emphasized is the nature of the determined constants. Indeed, they are not thermodynamic values but conditional constants. The determinations were carried out in 0.10 mol dm^{-3} KNO_3 medium, consequently in high concentration of NO_3^-. The medium was chosen taking into account the study of K. Bowman-James *et al.*[12] for a similar receptor $(H_6[24]mbz_2N_6)^{6+}$, see Scheme 1, for which a negligible association constant with nitrate was found. In two cases, for ph^{2-} and iph^{2-} anions, 0.10 mol dm^{-3} KCl was also used as medium for comparison. The values obtained are not conclusive, but the differences between corresponding constants in both media are very small, see Tables 2 and 4. Indeed, the main constant determined (corresponding to the formation of H_6LA^{4+}) is higher for ph^{2-} but slightly lower for iph^{2-} in KCl when compared to those obtained in KNO_3 medium. These results indicate that other factors derived from the nature of the anions and probably also the main type of interactions are also relevant. In a few other cases in which the effect of the electrolyte anion used to keep the ionic strength was taken into account,[12–14] the bulky sodium tosylate was used. However we ruled out this medium because ^{1}H NMR experiments revealed the significance of π–π stacking interactions involving the benzene rings of $(H_6Me_2[30]pbz_2N_6)^{6+}$, see below.

Table 3 Protonation constants (log $\beta_{H_hA_a}$) of ox^{2-}, mal^{2-}, suc^{2-}, $glut^{2-}$, $adip^{2-}$, bz^-, ph^{2-}, and iph^{2-}, and the corresponding stepwise constants, log K. T = 298.0 ± 0.1 K; I = 0.10 mol dm^{-3} in KNO_3[a]

Anion	Log β_1^H (or K_1^H)	Log β_2^H	Log K_2^H
ox^{2-}	3.81(1)	5.18(1)	1.37
mal^{2-}	5.23(1)	7.86(1)	2.63
suc^{2-}	5.23(1)	9.23(1)	4.00
$glut^{2-}$	5.01(1)	9.14(2)	4.13
$adip^{2-}$	5.01(1)	9.25(1)	4.24
bz^-	4.02(1)	—	—
ph^{2-}	5.00(1)	7.80(1)	2.80
	4.95(1)[b]	7.80(1)[b]	2.85[b]
iph^{2-}	4.27(1)	7.52(1)	3.25
	4.20(1)[b]	7.38(1)[b]	3.18[b]

[a] Values in parentheses are standard deviations on the last significant figures. A denotes the anion. [b] I = 0.10 mol dm^{-3} in KCl.

In Table 4 the associated constants for ox^{2-} with a related receptor, $(H_6[30]pbz_2N_6)^{6+}$, are also included.[15] The values are of the same order but slightly larger than those determined in the present work. The discrepancies arise more from the different protonation constants for the ligands and oxalic acid, see Tables 1 and 3, and also from the different work conditions, than from electronic or structural differences between the ligands.

The receptor $(H_6Me_2[30]pbz_2N_6)^{6+}$ can be visualized as composed by two different subunits: the benzene groups, responsible for the rigidity of the receptor, and the two triamine moieties, which have enough flexibility to adjust to the substrates. On the other hand, electrostatic and hydrogen-bonding interactions between the ammonium groups of the receptor and the oxygen atoms of the carboxylate moieties of the substrates are the only possible type of interactions between $(H_6Me_2[30]pbz_2N_6)^{6+}$ and the aliphatic substrates, while additional π–π stacking interactions can also be predicted between the benzene groups of the receptor and of the aromatic anions.

In the aliphatic series the flexibility and the overall basicity increase with the size of the methylenic chain between the two carboxylate groups, $glut^{2-}$ being however slightly less basic than suc^{2-}. The ox^{2-}, the shortest and more rigid of the series, has the strongest interaction with the receptor, however the value of the constant is too small to indicate a selective recognition. The aromatic substrates have larger association constants, see Fig. 3.

It is however interesting to observe that the constants for bz^- are not sensitive to pH variations, presenting values very similar in spite of the decrease of the positive charges of the receptor. This indicates that the binding of the anion occurs on one side of the molecule while the acid–base equilibria involve the amines at the opposite moiety of the molecule. In spite of this the RA_2 species was not found, probably because the two sides are sufficiently far away to act practically independently.

Table 4 Stepwise stability constants (log $K_{H_hL_lA_a}$) for the equilibria between the different protonated species of $(H_{6-i}Me_2[30]pbzN_6)^{(6-i)+}$ with ox^{2-}, mal^{2-}, suc^{2-}, $glut^{2-}$, $adip^{2-}$, ph^{2-}, iph^{2-}, and bz^-. L is the macrocyclic ligand $Me_2[30]pbzN_6$ and A the anion. I = 0.10 mol dm^{-3} in KNO_3 at 298.0 K

Equilibrium process	ox^{2-}	mal^{2-}	suc^{2-}	$glut^{2-}$	$adip^{2-}$	ph^{2-}	iph^{2-}	bz^-
$H_6L^{6+} + HA^- \rightleftarrows H_7LA^{5+}$	2.14, 2.12[a]	—	—	1.71	1.85	2.53, 2.69[b]	2.44, 2.72[b]	2.97
$H_6L^{6+} + A^{2-} \rightleftarrows H_6LA^{4+}$	2.71, 3.30[a]	2.21	2.23	2.19	2.06	3.15, 3.38[b]	3.05, 3.02[b]	2.94
$H_5L^{5+} + A^{2-} \rightleftarrows H_5LA^{3+}$	2.05, 2.72[a]	1.61	1.84	2.09	—	3.02, 3.05[b]	2.89, 2.68[b]	2.88
$H_4L^{4+} + A^{2-} \rightleftarrows H_4LA^{2+}$	—, 2.23[a]	—	1.64	1.69	—	2.69, 2.67[b]	2.76, 2.41[b]	2.82
$H_3L^{3+} + A^{2-} \rightleftarrows H_3LA^{+}$	—, —	—	—	—	—	2.30, 2.42[b]	2.46, —	—
$H_2L^{2+} + A^{2-} \rightleftarrows H_2LA$	—, —	—	—	—	—	—, 1.79[b]	2.20, —	—

[a] The receptor is $H_6[30]pbzN_6^{6+}$, I = 0.10 mol dm^{-3} in KCl, ref. 15. [b] This work, I = 0.10 mol dm^{-3} in KCl.

Another interesting point is related to the constants involving iph^{2-}, for which the values corresponding to the formation of the H_6LA^{4+}, H_5LA^{3+}, and H_4LA^{2+} are also unexpectedly very similar, nevertheless without structural information it is very difficult to interpret these features. Indeed the potentiometric technique does not give indications about the type of interaction or the sites of the receptor or the substrate involved in the association process. In order to obtain structural information about the association phenomena, ^{1}H NMR spectroscopic titrations and MD simulations were performed.

^{1}H NMR spectroscopy. The ^{1}H NMR spectroscopic titrations were performed in D_2O to be closer of the conditions used in the potentiometric studies, working at pH about 5 in order to centre the attention on the equilibrium reaction $H_6L^{6+} + A^{2-} \leftarrow H_6LA^{4+}$. The ionic strength was not controlled to avoid interfering anions. PF_6^-, as the receptor counterion, was chosen in order to obtain well-resolved ^{1}H NMR spectra.

In general the best technique to evaluate weak interactions (log $K \approx 4$) involves the addition of the substrate to the receptor,[16] however for the aromatic anions studied the opposite titration led to better results. As the aliphatic anions were used in their tetramethylammonium (TMA) form, and the intense TMA resonance is superimposed on the receptor H_c signal, data from this resonance were not obtained (for the numbering see Scheme 1). In Table 5 the chemical shifts (δ/ppm) of $(H_6Me_2[30]pbz_2N_6)^{6+}$ as well as the value of $\Delta\delta = (\delta_{receptor} - \delta_{obs})$ at the end of the titration are presented. For the aliphatic substrates only results for the ox^{2-} anion are shown. Indeed the shifts of the proton resonances of the receptor observed upon addition of the other aliphatic anions were too small to deserve a complete study, see Fig. 4.

Separated ^{1}H NMR signals were found for the receptor and the substrate protons upon formation of the receptor–substrate entity, indicating a fast exchange between the free and assembled molecules compared to the NMR time scale; see Fig. 5 for the case of addition of tph^{2-} anion.

The addition of ox^{2-} to a solution of $(H_6Me_2[30]pbz_2N_6)^{6+}$ leads to small upfield shifts of H_a, H_b, H_d and H_f resonances, and the other resonances do not exhibit coherent shifts, indicating that the aromatic moiety and the ammonium centres of the receptor are involved in the binding to ox^{2-}. Interactions of the type $-H_2N^+\cdots{}^-O_2C-$ were expected (electrostatic and H-bonding), but the contribution of the aromatic moieties is surprising, and in fact the shifts of the benzene proton resonance are larger than the others, see Table 5. These shifts can be explained by π–π stacking interactions of

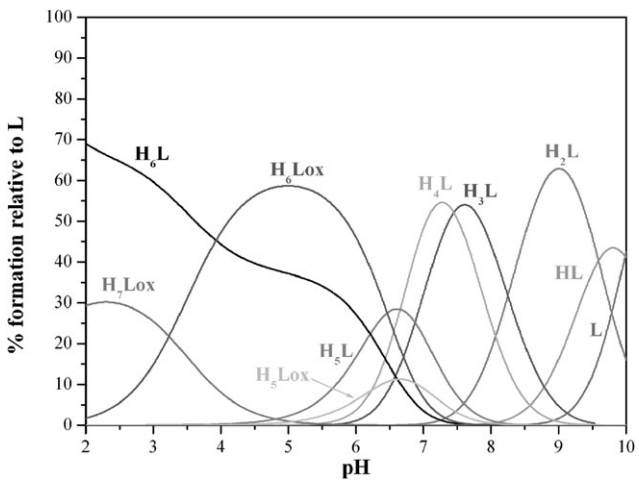

Fig. 1 Species distribution curves as a function of pH of the receptor $(H_6Me_2[30]pbz_2N_6)^{6+}$ in the presence of oxalate (ox^{2-}). L = $Me_2[30]pbz_2N_6$. Curves calculated for $C_{oxalate} = 3 \times C_{(H_6Me_2[30]pbz_2N_6)^{6+}}$. The charges of species were omitted.

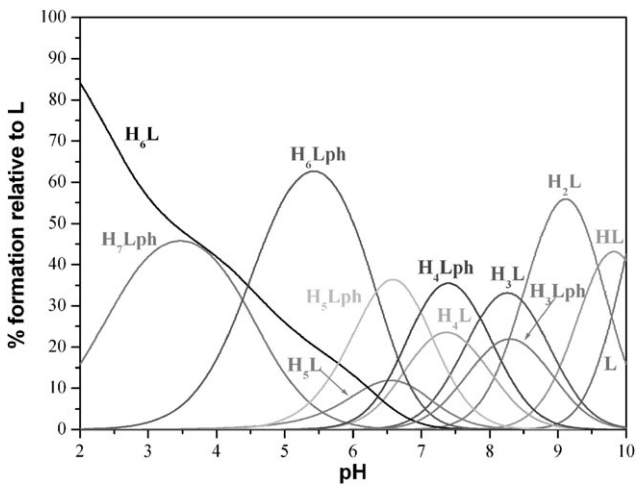

Fig. 2 Species distribution curves as a function of pH of the receptor $(H_6Me_2[30]pbz_2N_6)^{6+}$ in the presence of phthalate (ph^{2-}). L = $Me_2[30]pbz_2N_6$. Curves calculated for $C_{phthalate} = 3 \times C_{(H_6Me_2[30]pbz_2N_6)^{6+}}$. The charges of species were omitted.

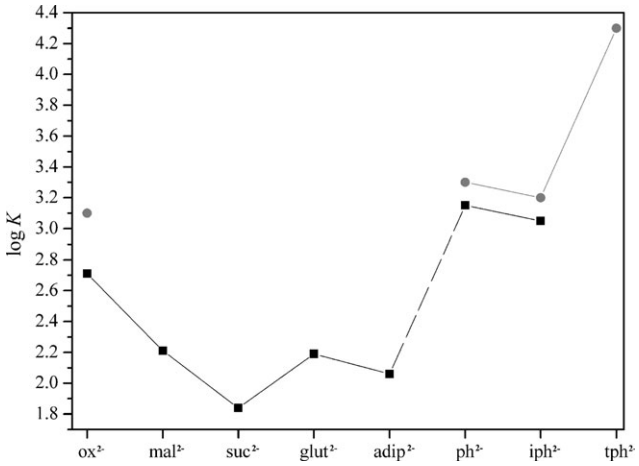

Fig. 3 Plot of log K, corresponding to the equilibrium reaction $H_6L^{6+} + A^{2-} \rightleftarrows H_6LA^{4+}$, as a function of the studied anions with different sizes and rigidities. The squares correspond to potentiometric and the circles to ^{1}H NMR measurements.

aromatic moieties of different receptor molecules or a completely different conformation of the aromatic rings of the receptor when the assembled molecule is formed. Unfortunately no single crystal adequate for X-ray diffraction determination of this supermolecule was obtained.

The addition of bz^{2-}, ph^{2-}, iph^{2-}, and tph^{2-} anions to the receptor causes upfield shifts of the proton resonances of the receptor which, in general, are larger than for ox^{2-}. However, chemical shift stabilization was not obtained even upon addition of 5 to 6 equivalents of anion solutions. In order to determine the association constants, titrations of anion solutions by addition of the protonated receptor were performed.

Table 5 ^{1}H NMR resonances (δ/ppm) and shifts ($\Delta\delta_{max} = \delta_R - \delta_{obs}$) for some proton resonances of the protonated macrocycle (R) upon addition of the substrate on saturation,[a] and the stepwise constants obtained

Anion		$\delta_{R^{6+}}$	δ_{RA}	δ_{RA_2}	$\Delta\delta_{max}$	log K_1	log K_2
ox^{2-}	H_a	7.528	7.501	—	0.027	3.1(1)	—
	H_b	4.286	4.262	—	0.024		
	H_f	2.879	2.859	—	0.020		
bz^-	H_b	4.286	4.283	4.254	0.032	2.9(1)	1.7(2)
	H_c	3.156	3.141	3.061	0.095		
	H_d	2.097	2.092	2.040	0.057		
	H_f	2.879	2.877	2.811	0.068		
ph^{2-}	H_a	7.528	7.524	7.483	0.045	3.3(1)	2.2(2)
	H_b	4.286	4.275	4.213	0.073		
	H_c	3.156	3.110	3.028	0.128		
	H_d	2.097	2.080	2.047	0.050		
	H_f	2.879	2.867	2.774	0.105		
iph^{2-}	H_a	7.528	7.450	7.348	0.180	3.2(1)	2.8(2)
	H_b	4.286	4.250	4.136	0.150		
tph^{2-}	H_a	7.528	7.500	7.415	0.108	4.3(2)	3.5(4)
	H_b	4.286	4.243	4.140	0.146		
	H_c	3.156	3.114	3.014	0.142		
	H_f	2.879	2.853	2.795	0.084		

[a] Proton resonances that have significant shifts upon addition of the substrate.

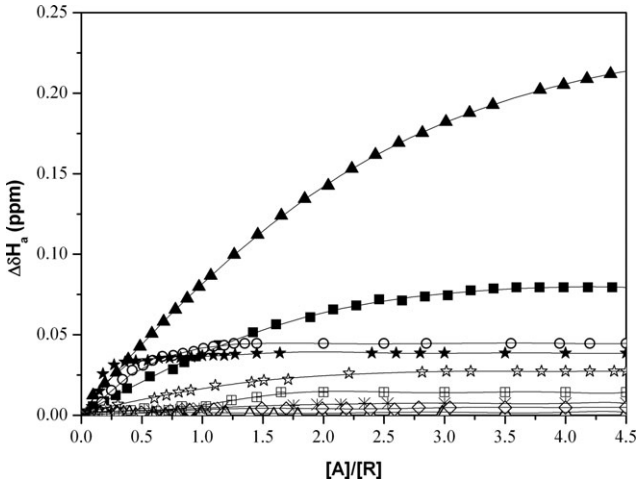

Fig. 4 ^{1}H NMR titration of $(H_6Me_2[30]pbz_2N_6)(PF_6)_6$ with several substrate anions, $\Delta\delta$ of the protons of the receptor as a function of the number of equivalents of substrate added, in D_2O following the singlet H_a of the receptor. The symbols for the anions are: ox^{2-} (☆), mal^{2-} (△), suc^{2-} (*), $glut^{2-}$ (⊞), $adip^{2-}$ (◇), bz^- (★), ph^{2-} (○), iph^{2-} (▲), and tph^{2-} (■).

Plots of $\Delta\delta$ as a function the $n_{receptor}/n_{substrate}$ ratio are shown in Fig. 6 (a) and (b).

The proton resonance shift pattern of the receptor is different in the titration of each aromatic anion indicating important structural differences in the assembled molecules. In all cases, except for bz^-, resonance H_e shifts downfield. Indeed, in the presence of iph^{2-} large shifts in H_a and H_b resonances were observed, and the other proton resonances only exhibit very small shifts. Accordingly, π–π stacking is the main expected interaction between the benzene rings of the receptor and iph^{2-}. However, the presence of ph^{2-} causes opposite features: shifts of H_c, H_f and H_d were observed, while H_a and H_b only undergo very small changes, indicating $-H_2N^+\cdots{}^-O_2C-$ as the main interactions. On the other hand, the presence of tph^{2-} results in simultaneous resonance shifts of the aromatic ring protons of the receptor, H_a and H_b, and also of H_c, H_d and H_f, implying π–π stacking, H-bonding

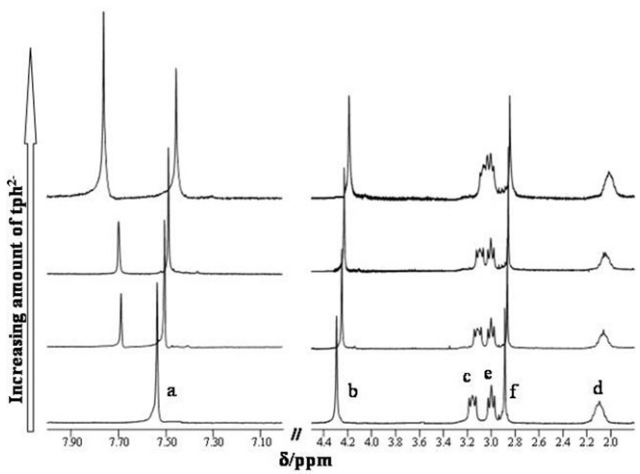

Fig. 5 ^{1}H NMR spectra for the titration of $(H_6Me_2[30]pbz_2N_6)(PF_6)_6$ receptor with tph^{2-} anion in D_2O.

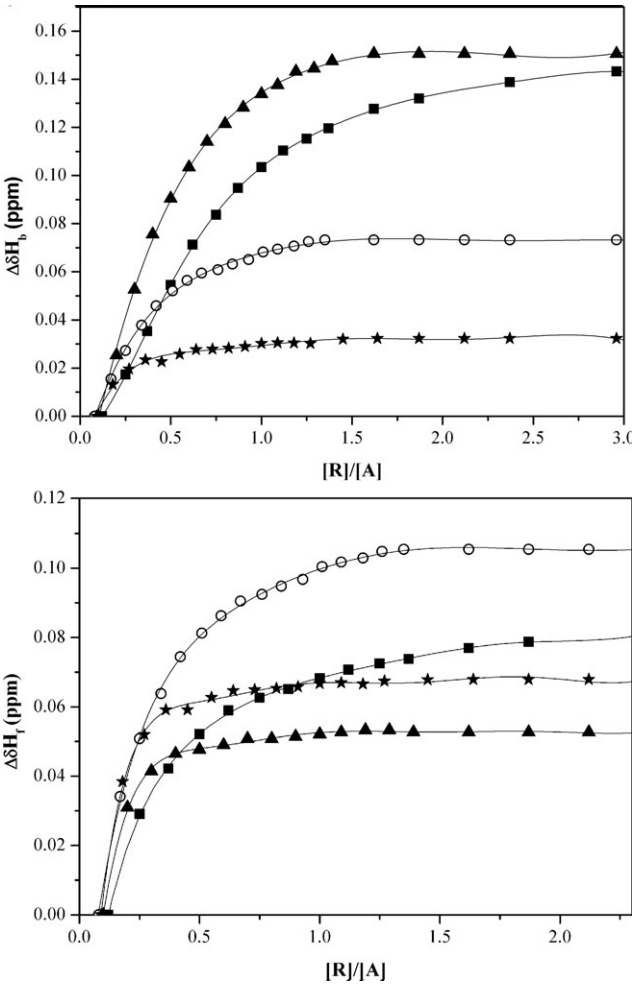

Fig. 6 ^{1}H NMR titration of $(H_6Me_2[30]pbz_2N_6)(PF_6)_6$ with aromatic anions, $\Delta\delta$ of the protons of the receptor as a function of the number of equivalents of receptor added, in D_2O following (a) the singlet H_b, and (b) the singlet of the $^+NCH_3$ (H_f) of the receptor. The symbols are bz^- (★), ph^{2-} (○), iph^{2-} (▲), and tph^{2-} (■).

and electrostatic interactions between substrate and receptor, suggesting a possible intercalation of tph^{2-} into the receptor backbone. The titration curves pattern corresponding to bz^- is similar to that observed for ph^{2-} but causing smaller shifts as expected from a monocarboxylate anion, indicating the same type of interactions.

The ^{1}H NMR titration data were also used to determine the association constants, using the HypNMR program.[17] The values obtained, compiled also in Table 5, have lower accuracy than those determined by potentiometry, because the titration was performed directly in the NMR tube in small volumes and by addition of very small amounts of titrants, and the ionic strength was not kept constant. The chemical shifts of the formed species are also indicated in Table 5.

Two species, RA and RA_2, were found for all the aromatic substrates, while for ox^{2-} only one constant was determined. In fact in the NMR conditions used it was possible to increase the amount of the aromatic substrates allowing the determination of K_2, while in our potentiometric conditions R : A ratios higher than 1 : 1 led to precipitation. In these conditions it was also possible to determine the association constants for the tph^{2-} substrate. The stepwise constants of Table 5 correspond to the following equilibrium reactions:

$$H_6L^{6+} + A^{2-} \rightleftarrows (H_6L)A^{4+} \qquad K_1$$

$$H_6L^{6+} + 2A^{2-} \rightleftarrows (H_6L)A_2{}^{2+} \qquad K_2$$

H_6L^{6+} being the receptor R and A the substrate.

The constants obtained by ^{1}H NMR titrations are slightly higher that those determined by potentiometry, but the experimental conditions were not the same. In fact the determinations were performed in D_2O, with no other anion at high concentration in solution, and PF_6^- was used as counterion. However a good agreement between the values obtained by both techniques was found, ox^{2-} exhibiting the largest divergence but within experimental errors due to the smaller $\Delta\delta$ values for this anion. As expected on the basis of the largest $\Delta\delta$ values and variety of interactions, tph^{2-} presents the highest association constants among the three aromatic dicarboxylate substrates. Ph^{2-} and iph^{2-} exhibit similar values by this technique, bz^- being the aromatic anion presenting the lowest values.

High or even very high values of association constants for dicarboxylate substrates with a variety of hexaammonium macrocycles or octaaza cryptands in water were reported.[14,15,18–27] In these selected cases only supermolecules with 1 : 1 R : A stoichiometry were found. X-Ray diffraction structures confirmed the inclusion of the substrates into the cavity of one cryptand with tph^{2-} [25] and another cryptand with ox^{2-}.[16] However, X-ray structures of hexaazamacrocyles with ox^{2-},[15,23] with iph^{2-} [27] and with tph^{2-} [27] showed that the respective substrates are intercalated rather than encapsulated into the cavity of the corresponding macrocycles.

Comparing our values with those of the literature it is possible to conclude that the $(H_6Me_2[30]pbz_2N_6)^{6+}$ is not a good receptor for aliphatic dicarboxylate substrates but it is a very interesting compound for the aromatic dicarboxylate anions, especially for tph^{2-}. The high value of the constant obtained for this assembled compound and, additionally, the indication from NMR data of the formation of strong and cooperative interactions, π–π stacking between the benzene rings of the receptor and of the tph^{2-}, Coulombic and hydrogen-bonding interactions between the carboxylate groups and ammonium moieties of the receptor, led us to predict that this substrate is included into the cavity of the receptor.

Molecular dynamics and free energy calculations

In order to bring further insight to the experimental binding studies, the interaction between $(H_6Me_2[30]pbz_2N_6)^{6+}$ receptor and the aromatic substrates ph^{2-}, iph^{2-}, and tph^{2-} was evaluated through molecular dynamics (MD) simulations and free energy calculations with the AMBER 8 suite of programs,[28] using the gaff force field.[29] The atomic point charges for the atoms in the protonated macrocycle and anions were calculated with the AM1-BCC method.[30] Molecular dynamics simulations were carried out in water boxes using as starting geometries for the complexes the lowest geometric arrangements found docking the receptor $(H_6Me_2[30]pbz_2N_6)^{6+}$ to each aromatic anion *via* molecular dynamics quenching

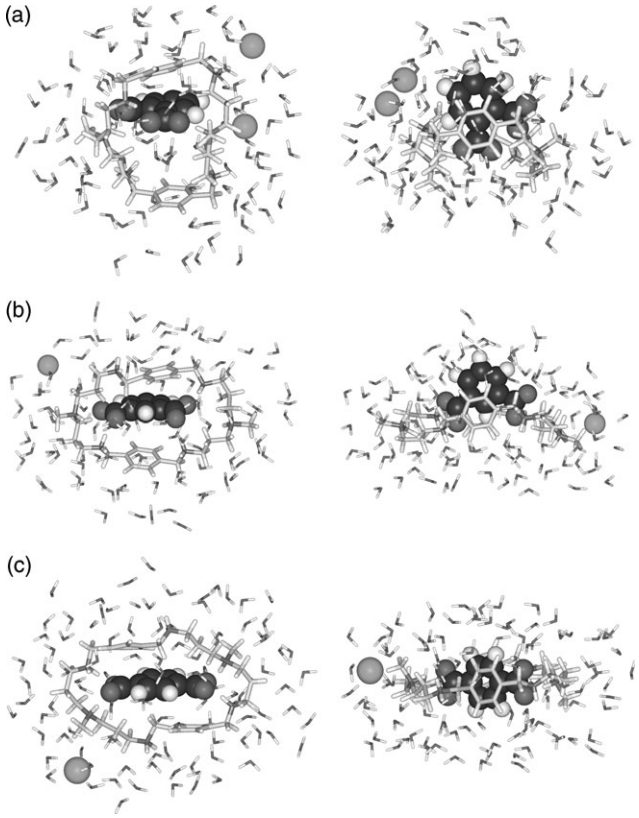

Fig. 7 Binding mode interactions between $(H_6Me_2[30]pbz_2N_6)^{6+}$ receptor and aromatic anions ph^{2-} (a), iph^{2-} (b), and tph^{2-} (c) in two different views. The macrocyclic cavity is emphasized in the left side and the spatial position of the substrate relative to the receptor is shown in the right side. The snapshots were taken after 7.1 ns of MD simulation with the first solvent shells composed of 100 water molecules. Only the chloride counterions inside the water shells are shown.

techniques as described below. Here is presented only the pertinent modelling results for the understanding of the substrate–receptor binding mode. The detailed description of this study will be published.[31] Snapshots taken after 7.1 ns of MD simulations illustrating the binding interaction between the $(H_6Me_2[30]pbz_2N_6)^{6+}$ receptor and ph^{2-}, iph^{2-}, and tph^{2-} anions are presented in Fig. 7 in two different views.

The ph^{2-} and iph^{2-} anions remained at the top of the macrocycle during the entire time of simulation. By contrast the tph^{2-} substrate enters into the macrocyclic cavity after *ca.* 1600 ps of simulation with formation of an inclusion complex.

The analysis of hydrogen bonds between the six potential N–H binding sites of the receptor and the four oxygen atoms from the carboxylate groups of each anion over the 9 ns of MD simulation was carried out using a cut-off of 2.5 Å for H···O distances and 120° for the N–H···O=C angles. The interaction between $(H_6Me_2[30]pbz_2N_6)^{6+}$ and the iph^{2-} anion involves mainly three N–H groups adjacent to the *p*-phenyl spacers and three oxygen atoms from the anion. These binding interactions are quite strong with average H···O distances in the range between 1.70 and 1.76 Å and average N–H···O=C angles from 166 to 171°. Furthermore one of these hydrogen bonds is kept continuously during a large simulation period leading to a lifetime of 411.9 ps.

The interactions of receptor with the ph^{2-} anion occur through three N–H binding sites and both oxygen atoms from two carboxylate groups forming five independent N–H···O=C hydrogen bonds with mean H···O distances ranging from 1.69 to 2.20 Å and mean N–H···O=C angles from 150 to 172°. Three hydrogen bonds involve the two N–H tertiary binding sites while the remaining two correspond to the interaction of a N–H secondary binding site with an oxygen atom from each one of the two carboxylate groups. The strongest hydrogen bond has a lifetime of 4.5 ns (H···O=1.69 Å and N–H···O=C 172°) and plays an important role in the interaction of the receptor with the ph^{2-} anion.

The molecular recognition of the tph^{2-} anion by $(H_6Me_2[30]pbz_2N_6)^{6+}$ involves four N–H binding sites, two N–H tertiary groups and two secondary ones and all the oxygen atoms from two carboxylate groups leading mainly to eight independent N–H···O=C hydrogen bonds. The H···O distances vary between 1.82 and 1.91 Å and the angles N–H···O=C range from 161 to 168°.

These MD simulations show that the molecular assembling between the receptor and these three aromatic anions requires the establishment of multiple and cooperative N–H···O=C hydrogen bonding interactions.[31] The pattern and number of hydrogen bonds depends of the relative position of the carboxylate groups on the benzene ring. The number of hydrogen bonds follow the order $iph^{2-} < ph^{2-} < tph^{2-}$. The encapsulation of thp^{2-} by the receptor determines the large number of N–H···O=C hydrogen bonds found. Furthermore, the assembled molecule $\{(H_6Me_2[30]pbz_2N_6)(tph)\}^{4+}$ is stabilized by π–π interactions between the benzene rings of the anion and the *p*-xylyl spacers of the receptor. After encapsulation the two benzene rings of the receptor remain almost parallel to the benzene ring of the substrate at interplanar distances consistent with the existence of this type of electrostatic interaction.

The average energetic and entropic contributions to the binding free energies of $(H_6Me_2[30]pbz_2N_6)^{6+}$ towards the aromatic anions ph^{2-}, iph^{2-}, and tph^{2-} are collected in Table 6 together with their standard errors. They were calculated with snapshots of the macrocyclic receptor, anionic substrate and complex taken from MD trajectories of three independent simulations using the MM-PBSA method.[32] Thus, MD simulations in explicit solvent were also carried out for the isolated anions and the macrocyclic receptor during 2 and 5 ns, respectively as described in the experimental section.

The relative binding energy (ΔG_{bind}) is negative in all cases indicating that the binding association between the receptor and each one of the anions ph^{2-}, iph^{2-}, and tph^{2-} is favourable. The theoretical values of −7.4 kcal mol^{-1} for tph^{2-}, −7.2 kcal mol^{-1} for ph^{2-}, and −7.6 kcal mol^{-1} for iph^{2-} are overestimated by 1.5, 2.6 and 3.2 kcal mol^{-1}, respectively, when compared with those calculated from ^1H NMR data. The deviations between the theoretical and experimental binding energies determined from potentiometric data are smaller. Indeed, the energetic difference decreases to −1.7 kcal mol^{-1} for iph^{2-} while the computed value for ph^{2-} is in a good agreement with the experimental one, the energetic difference being −0.3 kcal mol^{-1}. Therefore the binding affinities estimated from MD simulations reproduce well the experimental finding.

Table 6 Binding free energy contributions (kcal mol^{-1}) for the interactions of $(H_6Me_2[30]pbz_2N_6)^{6+}$ with the aromatic anions ph^{2-}, iph^{2-}, and tph^{2-}

	ph^{2-}		iph^{2-}		tph^{2-}	
Contribution[a]	Mean	σ[b]	Mean	σ	Mean	σ
ΔE_{elec}	−759.9	0.2	−753.4	0.2	−740.1	0.4
ΔE_{vdW}	−2.6	0.1	−5.2	0.1	−6.2	0.1
ΔE_{int}	4.6	0.2	2.0	0.1	6.2	0.2
ΔE_{MM}	−757.9	0.2	−756.6	0.2	−740.1	0.4
ΔG_{np}	−1.7	0.0	−1.8	0.0	−1.9	0.0
ΔG_{PB}	735.8	0.2	735.4	0.2	718.0	0.3
ΔG_{solv}	734.1	0.2	733.6	0.1	716.1	0.3
ΔG_{tot}	−23.8	0.1	−23.0	0.1	−24.0	0.1
$T\Delta S_{total}$	−16.6	0.0	−15.4	0.0	−16.6	0.0
ΔG_{bind}	−7.2	0.1	−7.6	0.1	−7.4	0.1

[a] Energy definitions: ΔE_{elec} = electrostatic energy; ΔE_{vdW} = van der Waals energy; E_{int} = internal strain energy. $\Delta E_{MM} = \Delta E_{elec} + \Delta E_{vdW} + \Delta E_{int}$; $\Delta G_{solv} = \Delta G_{np} + \Delta G_{PB}$, where ΔG_{np} = nonpolar solvation free energy and ΔG_{PB} = polar solvation free energy; $\Delta G_{tot} = \Delta G_{solv} + \Delta E_{MM}$; $\Delta G_{bind} = \Delta G_{tot} - T\Delta S_{total}$; [b] σ = standard errors of mean values.

The analysis of the free energy components shows that the electrostatic term is the largest contributor to the molecular mechanics internal energy. The Coulombic interactions favour the binding of the receptor to the ph^{2-} relative to the iph^{2-} and tph^{2-} anions by −6.5 and −19.8 kcal mol^{-1}, respectively. The electrostatic effect is partially compensated by the unfavourable polar term of the solvation energy. The solvation of the polar part of the assembled molecule $(H_6Me_2[30]pbz_2N_6)(tph)^{4+}$ requires *ca.* 17 kcal mol^{-1} less than the supermolecular associations with ph^{2-} and iph^{2-}, in which the anion is located outside of the macrocyclic cavity.[31] In water the total free energy ΔG_{tot} (the enthalpy, defined in Table 6) is −24.0, −23.8 and −23.1 kcal mol^{-1} for tph^{2-}, ph^{2-}, and iph^{2-}, respectively. These values are consistent with the affinity trend $tph^{2-} > ph^{2-} > iph^{2-}$ found from the experimental binding free energies. The formation of supramolecular associations between the receptor and the anions is disfavoured by the average entropic term by −16.6 kcal mol^{-1} for tph^{2-} and for ph^{2-}, and by −15.4 kcal mol^{-1} for iph^{2-}. The difference of 1.2 kcal mol^{-1} on the $T\Delta S$ term leads to a slightly lower binding free energy for the association with tph^{2-}. In other words, the binding affinity and the enthalpy of the receptor towards these three aromatic anions follow opposite trends.

The absolute free energies were also evaluated on the basis of a single trajectory file with snapshots of the anions and the receptor also taken from MD simulations carried out with the supermolecular associations. The average binding free energies found of −17.9 kcal mol^{-1} for tph^{2-}, −17.6 kcal mol^{-1} for ph^{2-}, and −16.0 kcal mol^{-1} for iph^{2-} are more negative than those calculated with snapshots extracted from separated trajectories, which indicates that the macrocycle receptor undergoes a conformational change upon anion binding accompanied by a free energy change (ΔG_{conf}) given by:

$$\Delta G_{conf} = \langle G_{mac}\,(\text{supermolecule trajectory})\rangle - \langle G_{mac}\,(\text{macrocycle trajectory})\rangle$$

where $\langle G_{mac}$ (supermolecule trajectory)$\rangle$ and $\langle G_{mac}$ (macrocycle trajectory)$\rangle$ are the average free energies for the macrocycle, calculated with snapshots extracted from the trajectories MD solution simulations performed in water with the supermolecule and the protonated macrocycle alone, respectively. The ΔG_{conf} for $(H_6Me_2[30]pbz_2N_6)^{6+}$ is 10.2 kcal mol^{-1} for the interaction with ph^{2-}, 10.3 kcal mol^{-1} with tph^{2-} and 8.5 kcal mol^{-1} with iph^{2-}. In all cases ΔG_{conf} is mainly determined by the enthalpic instead of the entropic term, which would be derived from a significant conformational change between the macrocycle in the supermolecule and in its free protonated state in water. In other words these results indicate that the $(H_6Me_2[30]pbz_2N_6)^{6+}$ receptor has a rigid and preorganized structure which experiences upon anion binding a slight conformational change induced mainly by the electrostatic bonding interactions, including the hydrogen bonds.

Conclusions

The molecular recognition ability of the ditopic receptor $(H_6Me_2[30]pbz_2N_6)^{6+}$ was evaluated towards a variety of aliphatic and aromatic carboxylate anions. The substrates differ in size, shape, rigidity and electronic properties. The binding studies were carried out by potentiometry and ^{1}H NMR spectroscopy in aqueous (or D_2O) solution. The first technique allowed the accurate determination of the association constants and the evaluation of all species that can be formed at different pH values, while the second technique complements these data with structural information. The ^{1}H NMR titrations have also shown that the studied receptor can assemble two molecules of the aromatic substrates, in an excess of anion, information that could not be obtained by the potentiometric studies due to solubility reasons. Additionally both techniques have good agreement in the association constant values determined in spite of the different working conditions.

The molecular recognition processes in water of the receptor $(H_6Me_2[30]pbz_2N_6)^{6+}$ with the three aromatic anions, ph^{2-}, iph^{2-}, and tph^{2-}, were theoretically evaluated by MD simulations and the corresponding binding energies were estimated using the MM-PBSA method. The pattern and the number of the hydrogen bonds reported by MD are consistent with the ^{1}H NMR data. The enthalpy contributions for the formation of supramolecular associations with these three anions are similar and consequently the binding affinities are the result of a delicate balance between entropic and energetic contributions. The binding free energies calculated with snapshots of the receptor, anion and supermolecules extracted from separated trajectory files are in reasonable agreement with experimental ones showing that the MM-PBSA method is a valuable tool to estimate in water the energy of binding between such highly charged species as the receptor $(H_6Me_2[30]pbz_2N_6)^{6+}$ and the aromatic anions ph^{2-}, iph^{2-}, and tph^{2-}.

The NMR and the theoretical studies suggest that the receptor has a clear preference for the tph^{2-} anion forming an inclusion supermolecule, while for the remaining anions the binding occurs outside of the macrocyclic cavity. The molecular recognition between the receptor and tph^{2-} is determined by the combination of electrostatic, hydrogen-bonding

and π–π interactions. Among the aliphatic series studied, the ox^{2-} substrate, having the smallest and rigid structure, shows the best binding.

Experimental

Microanalyses were carried out by the ITQB Microanalytical Service. The ^1H and ^{13}C NMR spectra were determined on a Bruker CXP 300 spectrometer. FAB mass spectra were recorded on an AutoSpecEQ mass spectrometer at University of Aveiro.

Reagents

Terephthaldialdehyde and *N*,*N*-bis(3-aminopropyl)methylamine were obtained from Aldrich. Oxalic acid (99.5%), malonic acid (>99%), adipic acid (extra pure) and succinic acid (99%) were purchased from Merck. Terephthalic acid (98%), glutaric acid (99%), phthalic acid (>99.5%) and isophthalic acid (99%) were purchased from Aldrich. All chemicals were of reagent grade and used as supplied. The reference used for the ^1H NMR measurements in D_2O was 3-(trimethylsilyl)propanoic acid-d_4 sodium salt. For ^{13}C NMR spectra dioxane was used as an internal reference. The ligand $Me_2[30]pbz_2N_6$ was synthesized according to the literature.[6] The hexaprotonated form of the ligand $(H_6Me_2[30]pbz_2N_6)(PF_6)_6$ was prepared by dissolving $Me_2[30]pbz_2N_6$ in water (10 cm^3) and adjusting the pH to 4.5 by addition of hexafluorophosphoric acid (60 wt% in water) from Aldrich. The solution was stirred overnight and then the pH adjusted again. The solution was evaporated to dryness and the solid recrystallized from ethanol and dried under vacuum before use. $(H_6Me_2[30]pbz_2N_6)(PF_6)_6$: ^1H NMR (D_2O): δ 2.097 (8 H, q, $NCH_2CH_2CH_2N$), 2.879 (6 H, s, NCH_3), 3.016 (8 H, t, $NCH_2CH_2CH_2N$), 3.156 (8 H, t, $NCH_2CH_2CH_2N$), 4.286 (8 H, s, $bzCH_2N$) and 7.528 (8 H, s, bz). FAB MS: *m*/*z* 496 $[HL^+]$, 641 $[HL^+ + PF_6^-]$, 786 $[HL^+ + 2PF_6^-]$, 931 $[HL^+ + 3PF_6^-]$, 1076 $[HL^+ + 4PF_6^-]$, 1221 $[HL^+ + 5PF_6^-]$, 1366 $[HL^+ + 6PF_6^-]$.

Potentiometric measurements

Reagents and solutions. Anions were prepared from the respective acids by addition of two equivalents of KOH in aqueous solution. The solutions were evaporated and the solids recrystallized from acetone. The anions were then standardized by titration using a standard HNO_3 solution. Except for the aliphatic acids where a solution of the acid was prepared and then standardized by titration using a standard KOH solution. A carbonate-free solution of the titrant, KOH, was freshly prepared, maintained in a closed bottle, and discarded when the percentage of carbonate was about 0.5% of the total amount of base (tested by the Gran method).[33,34] The demineralized water used was obtained from a Millipore/Milli-Q system.

Equipment and working conditions. The equipment used was described before.[6] The temperature was kept at 25.0 ± 0.1 °C; atmospheric CO_2 was excluded from the cell during the titration by passing purified argon across the top of the solution in the reaction cell. The ionic strength of the solutions was kept at 0.10 mol dm^{-3} KNO_3 or KCl.

Measurements. The $[H^+]$ of the solutions was determined by the measurement of the electromotive force of the cell, $E = E'^\circ + Q\log[H^+] + E_j$. E'°, Q, E_j and $K_w = ([H^+][OH])$ were obtained as described previously.[6] The term pH is defined as $-\log [H^+]$. The value of K_w was found to be equal to $10^{-13.80}$ mol^2 dm^{-6}. The potentiometric equilibrium measurements were carried out using 20.00 cm^3 of $\cong 2.09 \times 10^{-3}$ mol dm^{-3} $Me_2[30]pbz_2N_6$ solutions diluted to a final volume of 30.00 cm^3, in the absence of dicarboxylate anions, then in the presence of each anion at 1 : 0.5 and 1 : 1 $C_L : C_A$ ratios for the aromatic anions, and 1 : 1, 1 : 2 and 1 : 4 $C_L : C_A$ ratios for the aliphatic series.

Calculation of equilibrium constants. Overall protonation constants, β_i^H, were calculated by fitting the potentiometric data obtained for all the performed titrations with the HYPERQUAD program.[10] The protonation constants of the studied anions were also determined from the experimental data in the same experimental conditions, also using the HYPERQUAD program. All these constants were taken as fixed values to obtain the equilibrium constants of the new species from the experimental data corresponding to all the titrations at different R : A stoichiometries, also using the HYPERQUAD program. The initial computations were obtained in the form of overall stability constants, $\beta_{H_hL_lA_a}$ values, $\beta_{H_hL_lA_a} = [H_hL_lA_a]/[H]^h[L]^l[A]^a$. The errors quoted are the standard deviations of the overall stability constants given directly by the program for the input data, which include all the experimental points of all titration curves. The species considered in a particular model were those that could be justified by the principles of supramolecular chemistry.

The stability constants for $(H_6Me_2[30]pbz_2N_6)^{6+}$ and the different anions were determined from a minimum of 150 (for bz^-) to 265 (for ox^{2-}) experimental points, and a minimum of two titration curves, except for adipate for which only 60 experimental points were considered.

NMR studies

Reagents and solutions. Potassium salts of each anion were prepared by neutralization of the respective acid with potassium hydroxide in water, followed by recrystallization with acetone–ethanol. The solids were dried under vacuum before use. A solution of NaOH (0.100 mol dm^{-3}) was prepared from standard ampoules from Aldrich. The acids (from Aldrich) were used without further purification. Tetramethylammonium salts of the aliphatic anions, $(TMA)_2$aliphatic, were prepared in similar way. Solutions of the $(H_6Me_2[30]pbz_2N_6)(PF_6)_6$ (3.0–7.0 × 10^{-3} mol dm^{-3} and 15.0–28.0 × 10^{-3} mol dm^{-3}) were prepared by dissolution of the macrocycle in 0.5 and 1.0 cm^{-3} of D_2O, respectively. The anion solutions were prepared from 18.0–30.0 × 10^{-3} mol dm^{-3} and 1.5–8.0 × 10^{-3} mol dm^{-3} by dissolution of the potassium or TMA salts in 0.5 and 1.0 cm^{-3} of D_2O, respectively. The initial ^1H NMR spectrum was recorded without anion (or receptor) present, and then aliquots of receptor (or anion) salt solutions were added using a Hamilton syringe (Microliter 700 series of 25 μL) or a micropipette of 250 μL (EDP-2). About 15 to 30 additions were necessary for each

titration until no further change in the chemical shift was observed. All measurements were done at 300 K.

A Bruker CXP 300 spectrometer was used to perform the ^{1}H NMR spectra, and each solution was left 20 to 30 min to stabilize. No effort was made to maintain the ionic strength constant to avoid competition of other anions.

Changes in the chemical shift of all the protons, except the H_c proton in the aliphatic anion titrations, were recorded. The association constants of the various species formed in solution were determined from the experimental titration data using HypNMR,[17] which requires as input the concentration of each component and the observed chemical shift. The fitting included the binding constants and the chemical shift of each $R:A_i$ species. Initial calculations provided overall stability constants, $\beta_{R_rA_a}$ values, $\beta_{R_rA_a} = [R_rA_a]/[R]^r[A]^a$. RA and RA_2 species were found in most cases. Differences between the values of log β_{RA_2} and log β_{RA} provide the stepwise reaction constants. The errors quoted are the standard deviations of the overall stability constants given directly by the program from the input data, including the experimental points for all resonances of the titration curves. The standard deviations of the stepwise constants were determined by the normal propagation rules.

Molecular modelling studies

All molecular modelling simulations and subsequent free energy calculations were carried out with the AMBER 8 suite of programs,[28] using the gaff force field.[29]

The initial coordinates of the $(H_6Me_2[30]pbz_2N_6)^{6+}$ receptor were generated from the crystal structure of the free macrocycle[6] adding six protons to N–H binding sites, while the structures of the ph^{2-}, iph^{2-}, and tph^{2-} dicarboxylate guests were built in the Cerius-2 software package.[35] The atomic charges of all species were calculated with the AM1-BCC charge model[30] using the Antechamber module. The docking between the receptor and each one of the anions was performed through the quenching molecular dynamics. The anion molecule was positioned above the macrocyclic cavity and the model complex was energy minimized by molecular mechanics. The minimized structure was then subject in gas phase to a molecular dynamic quenching run at 2000 K using a time step of 1 fs. 20 000 conformations were generated at 0.1 ps intervals and they were minimized by molecular mechanics with the Sander module *via* conjugate gradients until a convergence using an appropriated house script. The energetic convergence criterion was 0.0001 kcal mol^{-1}. The lowest energy geometric arrangements found for the supramolecular associations of $(H_6Me_2[30]pbz_2N_6)^{6+}$ with ph^{2-}, iph^{2-}, and tph^{2-} anions were solvated with 1460 TIP3P water molecules[36] to fill cubic boxes. Four chloride anions were placed outside of the receptor to balance the charges. The systems were equilibrated under periodic boundary conditions using the following multistage protocol. The equilibration process started with the minimization of water molecules and Cl^- counterions by molecular mechanics with 1000 steps by the steepest descent method followed by 10 000 steps of conjugate gradients keeping the structure of the supermolecular association receptor–anion rigid with positional restrains of 500 kcal mol^{-1} Å^{-2}. After minimization, the solvated system was heated up to 300 K over 50 ps using an NVT ensemble. Then, the positional restrain was removed and solvent density was adjusted at an average pressure of 1 atm through a MD simulation run with length enough (typically 400 ps) to adjust the density of the cubic box to the expected value for liquid water at room temperature. At this stage the average value for density remained constant, at least during the last 100 ps of NPT simulation. Finally, data collection runs in an NPT ensemble at 300 K and 1 atm were carried out over 9 ns from the equilibrated structures of the solvated supermolecules. Snapshots were saved every 0.2 ps. Bond lengths involving all bonds to hydrogen atoms were constrained with the SHAKE algorithm.[37] The Particle Mesh Ewald method[38] was used to treat the long-range electrostatic interactions and the non-bonded van der Waals interactions were truncated with a 12 Å cut-off. MD simulations in explicit solvent were also carried out for the isolated anions and the free protonated macrocycle following a protocol similar to that adopted for the simulations performed with the assembled molecules. The anions and the protonated macrocycle were immersed in a cubic boxes composed of 884 and 1660 TIP3P water molecules,[36] respectively. The electrostatic neutrality of these periodic systems was obtained adding six chloride anions to the periodic box of the macrocycle receptor and two sodium cations to the periodic boxes of the anions. Data collection runs of 5 and 2 ns were carried out for protonated receptor and isolated anions, respectively.

The binding free energy terms, listed in Table 6, for each supramolecular entity, were calculated by post-processing the trajectories of three independent simulations done for the supermolecule, anion and receptor with the MM-PBSA method.[32] Snapshots of individual species with solvent removed were taken from the corresponding MD trajectory files at intervals of 1 ps leading to a total of 9000, 5000 and 2000 frames for the complex, the macrocyclic receptor and the anions, respectively. Molecular mechanical gas-phase energies, solvation free energies and entropies were determined for each snapshot followed by averaging the energy values. The solvation free energies were calculated using a continuum representation of the solvent with the first term (G_{PB}) estimated solving the Poisson–Boltzmann equation for zero salt concentration and the second one (G_{np}) determined from the solvent accessible area. The entropic contribution was estimated *via* the normal mode analysis. A more detailed description of the experimental procedure will be published elsewhere.[31]

Acknowledgements

The authors acknowledge the financial support from Fundação para a Ciência e a Tecnologia (FCT) and POCTI, with coparticipation of the European Community fund FEDER (Project n. POCTI/1999/QUI/35396). Sílvia Carvalho also acknowledges FCT for the grant (SFRH/BD/13793/2003).

References

1 *Supramolecular Chemistry of Anions*, ed. A. Bianchi, K. Bowman-James and E. Garcia-España, Wiley-VCH, New York, 1997.

2 R. J. Fitzmaurice, G. M. Kyne, D. Douheret and J. D. Kilburn, *J. Chem. Soc., Perkin Trans. 1*, 2002, 841.
3 J. M. Llinares, D. Powell and K. Bowman-James, *Coord. Chem. Rev.*, 2003, **240**, 57.
4 C. R. Bondy and S. J. Loeb, *Coord. Chem. Rev.*, 2003, **240**, 77.
5 (*a*) P. A. Gale, *Coord. Chem. Rev.*, 2000, **199**, 181; (*b*) P. A. Gale, *Coord. Chem. Rev.*, 2001, **213**, 79; (*c*) P. A. Gale, *Coord. Chem. Rev.*, 2003, **240**, 191.
6 S. Carvalho, C. Cruz, R. Delgado, M. G. B. Drew and V. Félix, *Dalton Trans.*, 2003, 4261.
7 M. Pietraszkiewicz, O. Pietraszkiewicz, K. Bujno and R. Bilewicz, *Pol. J. Chem.*, 1998, **72**, 852.
8 C. Anda, A. Llobet, A. E. Martell, B. Donnadieu and T. Parella, *Inorg. Chem.*, 2003, **42**, 8545.
9 P. Arranz, A. Bencini, A. Bianchi, P. Diaz, E. García-España, C. Giorgi, S. V. Luis, M. Querol and B. Valtancoli, *J. Chem. Soc., Perkin Trans. 2*, 2001, 1765.
10 P. Gans, A. Sabatini and A. Vacca, *Talanta*, 1996, **43**, 1739.
11 L. D. Pettit and K. J. Powell, *IUPAC Stability Constants Database*, Academic Software, Sourby Old Farm, Timble, Ottley, Yorks, UK, 2004, E-mail: scdbase@acadsoft.co.uk.
12 T. Clifford, A. Danby, J. M. Llinares, S. Mason, N. W. Alcock, D. Powell, J. A. Aguilar, E. García-España and K. Bowman-James, *Inorg. Chem.*, 2001, **40**, 4710.
13 B. Dietrich, J. Guilhem, J.-M. Lehn, C. Pascard and E. Sonveaux, *Helv. Chim. Acta*, 1984, **67**, 91.
14 M. W. Hosseini and J.-M. Lehn, *Helv. Chim. Acta*, 1988, **71**, 749.
15 C. Anda, A. Llobet, A. E. Martell, J. Reibenspies, E. Berni and X. Solans, *Inorg. Chem.*, 2004, **43**, 2793.
16 J. Nelson, M. Nieywenhuyzen, I. Pál and R. M. Town, *Dalton Trans.*, 2004, 2303.
17 C. Frassineti, S. Ghelli, P. Gans, A. Sabatini, M. S. Moruzzi and A. Vacca, *Anal. Biochem.*, 1995, **231**, 374.
18 B. Dietrich, M. W. Hosseini, J.-M. Lehn and R. B. Sessions, *J. Am. Chem. Soc.*, 1981, **103**, 1282.
19 M. W. Hosseini and J.-M. Lehn, *J. Am. Chem. Soc.*, 1982, **104**, 3525.
20 M. W. Hosseini and J.-M. Lehn, *Helv. Chim. Acta*, 1986, **69**, 587.
21 A. E. Martell and R. J. Motekaitis, *J. Am. Chem. Soc.*, 1988, **110**, 8059.
22 R. J. Motekaitis and A. E. Martell, *Inorg. Chem.*, 1992, **31**, 5534.
23 Q. Lu, R. J. Motekaitis, J. J. Reibenspies and A. E. Martell, *Inorg. Chem.*, 1995, **34**, 4958.
24 J. Nelson, M. Nieuwenhuyzen, I. Pál and R. M. Town, *Dalton Trans.*, 2004, 229.
25 J.-M. Lehn, R. Méric, J.-P. Vigneron, I. Bkouche-Waksman and C. Pascard, *J. Chem. Soc., Chem. Commun.*, 1991, 62.
26 M. Dhaenens, J.-M. Lehn and J.-P. Vigneron, *J. Chem. Soc., Perkin Trans. 2*, 1993, 1379.
27 T. Paris, J.-P. Vigneron, J.-M. Lehn, M. Cesario, J. Guilhem and C. Pascard, *J. Inclusion Phenom. Macrocyclic Chem.*, 1999, **33**, 191.
28 D. A. Case, T. A. Darden, T. E. Cheatham III, C. L. Simmerling, J. Wang, R. E. Duke, R. Luo, K. M. Merez, B. Wang, D. A. Pearlman, M. Crowley, S. Brozell, V. Tsui, H. Gohlke, J. Mongan, V. Hornak, G. Cui, P. Beroza, C. Schafmeister, J. W. Caldwell, W. S. Ross and P. A. Kollman, *AMBER version 8*, University of California, San Francisco, 2004.
29 J. Wang, R. M. Wolf, J. W. Caldwell, P. A. Kollmann and D. A. Case, GAFF force field, *J. Comput. Chem.*, 2004, **25**, 1157.
30 A. Jakalian, B. L. Bush, D. B. Jack and C. I. Bayly, *J. Comput. Chem.*, 2000, **21**, 132.
31 N. Fonseca, S. Carvalho, R. Delgado, P. J. A. Ribeiro-Claro and V. Félix, unpublished results.
32 P. A. Kollman, I. Massova, B. Kuhn, S. Huo, L. Chong, M. Lee, T. Lee, Y. Duan, W. Wang, O. Donni, P. Cieplak, J. Srinivasan, D. A. Case and T. E. Cheatham III, *Acc. Chem. Res.*, 2000, **33**, 889.
33 G. Gran, *Analyst*, 1952, **77**, 661.
34 F. J. Rossotti and H. J. Rossotti, *J. Chem. Educ.*, 1965, **42**, 375.
35 *CERIUS2 version 4.2*, Molecular Simulations Inc., San Diego, 2000.
36 W. L. Jorgensen, J. Chandrasekhar, J. D. Madura, R. W. Impey and M. L. Klein, *J. Chem. Phys.*, 1983, **79**, 926.
37 J. P. Ryckaert, G. Cicotti and H. J. C. Berendsen, *J. Comput. Phys.*, 1977, **23**, 327.
38 U. Essmann, L. Perera, M. L. Berkowitz, T. Darden, H. Lee and L. G. Perdensen, *J. Chem. Phys.*, 1995, **103**, 8577.